

## **Parametric Study of Plain Fin and Tube Evaporator Using CO<sub>2</sub> as A Refrigerant**

Ashish D. Kadam<sup>1</sup>, Dr. Atul S. Padalkar<sup>2</sup>, Avadhoot V. Wale<sup>3</sup>

<sup>1</sup> *Sinhgad College of Engineering, Vadgaon (Bk.), Pune*

<sup>2</sup> *Flora Institute of Technology, Pune*

<sup>3</sup> *Sinhgad College of Engineering, Vadgaon (Bk.), Pune*

---

**Abstract**—At the turn of the century, annual fluorocarbon refrigerant emissions from mobile and unitary air-conditioning equipments is likely to pass 100,000 metric tonnes, corresponding to a global warming impact of more than 150 million metric tonnes of CO<sub>2</sub>. Even larger indirect CO<sub>2</sub> emissions result from the generation of power to drive the systems. With its use of a non-flammable and non-toxic natural fluid, the transcritical CO<sub>2</sub> system is a primary candidate for next-generation air-conditioning systems. This motivated the authors to design a CO<sub>2</sub> air-conditioning system. In this paper, the authors present Effectiveness-NTU method of thermal design of a plain-fin and tube evaporator for CO<sub>2</sub> air-conditioning system. Using Engineering Equation Solver, the authors have proposed an optimum design of the CO<sub>2</sub> evaporator by parametric optimization. Generally CO<sub>2</sub> heat exchangers are designed for high refrigerant mass flux and use small-diameter tubes or extruded flat micro-channel tubes. The designed plain-fin and tube evaporator uses 3/16" OD tubes giving near-mini channel effect. Achieving sufficient compactness of 787m<sup>2</sup>/m<sup>3</sup> this evaporator is capable of giving 2.2 kW of cooling effect. For CO<sub>2</sub>, refrigerant-side heat transfer coefficients are higher than with fluorocarbons, and reduced internal surface areas can therefore be tolerated. In current design, the authors achieved around 7,500 W/m<sup>2</sup>-K of CO<sub>2</sub> heat transfer coefficient.

**Keywords**—Global Warming, Natural Refrigerants, Transcritical CO<sub>2</sub> System, Compact Heat Exchangers, Plain-Fin And Tube Evaporator.

---

### **I. INTRODUCTION**

Though being one of the first refrigerants to be used in compression type refrigerating machines, CO<sub>2</sub> rapidly eclipsed as a refrigerant post World War II. This is because the advent of synthetic halocarbon refrigerants, which were addressed as safe and ideal refrigerants at that time. The stratospheric Ozone depletion and global warming issue led to phasing out of CFC and HCFC working fluids through the Montreal protocol. The new HFC fluids as substitute refrigerants are subject to regulations under the Kyoto Protocol because of their high global warming potential. In this mixed situation, CO<sub>2</sub> is being revisited as a fully environment friendly refrigerant [1]. Apart from being a natural substance, CO<sub>2</sub> also has various advantages as listed below.

1. It is non-flammable and non-toxic, inexpensive and widely available.
2. Low global warming potential unlike synthetic refrigerants.
3. Low vapor to liquid density ratio.
4. High volumetric heat capacity and high heat transfer coefficient.
5. Low saturation temperature gradient, better than R134a and R22.

All these pro-environment properties make CO<sub>2</sub> a promising refrigerant in today's global warming scenario. Heat exchangers for mobile and unitary equipment are designed with a finned air-side surface and usually have more than 700 m<sup>2</sup> surface area per m<sup>3</sup> core volume. This ratio is the loosely defined limit for a compact heat exchanger. The heat exchangers may be mechanically expanded tube-in-fin units or brazed aluminum cores, in both cases various enhancements are used on the air and refrigerant sides. The high working pressure and favorable heat transfer properties of CO<sub>2</sub> enable reduced tube diameters and small refrigerant-side surface areas. Since these reductions may give room for more air-side surface per unit core volume, the compactness can be increased [4].

The scope of the present paper is to discuss the thermal design and development of compact plain-fin and tube evaporator for transcritical CO<sub>2</sub> air conditioning system suitable for Indian subtropical conditions.

### **II. LITERATURE REVIEW**

The plain-fin and tube heat exchangers are usually less expensive on a unit heat transfer surface area basis due to their simple and mass-production construction features. In the current energy conservation era, plain-fin and tube geometry is becoming widespread, since the bond between the fin and tube is made by mechanically or hydraulically expanding the tube against the fin. This method is energy efficient compared to employing welding, brazing, or soldering. Despite the limitation on operating temperature imposed by mechanical bond, the plain-fin and tube exchangers can withstand ultrahigh pressures on the tube side, although the highest temperature is again limited by the type of bonding, materials used, and material thickness.

Air-conditioning systems based on CO<sub>2</sub> operate mostly in a transcritical cycle, i.e. with supercritical high-side pressure and subcritical low-side conditions. Heat rejection takes place by cooling of the single-phase high-pressure fluid and not by condensation as in conventional systems. Heat is absorbed by evaporation, but the evaporating pressure is quite high. Typical low-side reduced pressures with CO<sub>2</sub> are between 0.5 and 0.7 in air-conditioning applications, as compared with around 0.1 for HFC/HCFC fluids. The effects on refrigerant properties and heat transfer characteristics by supercritical or near-critical operation are quite important for optimal heat exchanger design [4].

Typical CO<sub>2</sub> evaporator pressures range from 35 to 70 bar, which is about 10 times the pressures for conventional refrigerants. Fluid properties and optimum refrigerant-side mass flux and pressure drop therefore differ from conventional data. Comparisons between properly designed CO<sub>2</sub> evaporators and baseline HFC/HCFC evaporators show that, although the pressure level is much higher with CO<sub>2</sub>, the explosion energy (product of pressure and volume) is similar, since the internal volume is greatly reduced in CO<sub>2</sub> units [4].

The high thermal conductivity, low kinematic viscosity and high specific heat of liquid CO<sub>2</sub> are favorable for heat transfer behavior. A low liquid/vapor density ratio may give less problems of distribution in CO<sub>2</sub> evaporators, since the two-phase flow is likely to behave more homogeneously than with low-pressure refrigerants. Reduced surface tension may improve the evaporation heat transfer coefficient in certain boiling regimes [4]. Measured heat transfer coefficients for in-tube evaporation of pure CO<sub>2</sub> are generally about twice the predicted coefficients derived from existing correlations [4]. One possible reason is that existing correlations, such as the ones by Shah, Gungor and Winterton, or Steiner and Ozawa, do not account for variation of liquid surface tension [4]. The experimental data published by Bredesen et al. are based on larger tube diameter and lower heat and mass flux than what is relevant for compact air-conditioning evaporators. Even so, the measurements show heat transfer coefficients as high as 8-14 kW/m<sup>2</sup>-K for a heat flux of 6-9 kW/m<sup>2</sup> and a mass flux of 200-400 kg/m<sup>2</sup>-s [4].

The two-phase flow characteristics of CO<sub>2</sub>, such as flow pattern, flow boiling heat transfer and two-phase pressure drop are quite different unlike conventional refrigerants. Flow patterns being important in study of very complex two-phase flow phenomena and heat transfer trends in flow boiling, Cheng et al. [5] developed a flow pattern based flow boiling heat transfer model. Although their model is limited by its parameter ranges, it relates the flow patterns to the corresponding heat transfer mechanisms. Thus, it is different from the numerous empirical models, such as the correlations [6] of Chen, Shah, Gungor and Winterton, Kandlikar, Liu and Winterton etc., which do not include flow pattern information.

As a result, a new general flow boiling heat transfer model was developed by Cheng et al. [6] by modifying the Cheng et al. [5] heat transfer model. The heat transfer model for CO<sub>2</sub> developed by Cheng et al. [6] covers all flow regimes and is applicable to a wider range of conditions: tube diameters - 0.6 to 10 mm, mass velocities - 50 to 1500 kg/m<sup>2</sup>-s, heat fluxes - 1.8 to 46 kW/m<sup>2</sup> and reduced pressures - 0.21 to 0.87. To validate their results, Cheng et al. [6] compared their heat transfer model to an extensive experimental database and found a good agreement between the predicted and experimental data in general within  $\pm 30\%$ .

Cheng et al. [7] found that the leading pressure drop prediction methods - the correlations by Chisholm, Friedel, Grönnerud, Müller-Steinhagen and Heck, a modified Chisholm correlation by Yoon et al., and the flow pattern based model of Moreno Quibén and Thome etc, do not work well for CO<sub>2</sub>. The reason for this the authors [5] say is that, these methods do not usually cover the much lower liquid-to-vapor density ratios, very small surface tension characteristic of CO<sub>2</sub> at high pressures, and do not usually contain any flow pattern information intrinsically related to the two-phase frictional pressure drop. Hence, Cheng et al. [5] incorporated the updated CO<sub>2</sub> flow pattern map, and modified the model of Moreno Quibén and Thome developed for R-22, R-410a and R-134a, using the CO<sub>2</sub> pressure drop database. Compared to Friedel [13] method, Cheng et al. [7] found that their new two-phase frictional pressure drop model for CO<sub>2</sub>, predicts most of the macro-scale and micro-scale channel pressure drop data within  $\pm 30\%$ , with smaller standard deviation and mean error.

In many situations, refrigerant circuiting and mass flux for an evaporator can be optimized on the basis of a maximum tolerable saturation temperature drop (due to pressure drop) at constant outlet pressure. The tolerable pressure drop then depends on the slope of the saturation pressure curve. At 0°C, for instance, refrigerants like HCFC-22 and HFC-134a allow a pressure drop of 0.1 bar per K temperature drop, while a CO<sub>2</sub> evaporator can tolerate nine times higher pressure drop for the same loss in temperature [4]. The effects of some of the above factors - heat transfer coefficients, pressure drops, vapour density and slope of saturation pressure curve - are illustrated by the following example [4].

An evaporator tube for HFC-134a was specified, having an ID of 12.0 mm and a length of 20 m. For a friction and acceleration pressure drop giving 1 K temperature drop, and 0°C saturated vapor outlet, a cooling capacity of 1.6 kW was estimated [4]. A CO<sub>2</sub> evaporator tube with equal length and capacity for the same temperature drop was designed by varying the mass flow rate and tube diameter. By reducing the ID of the CO<sub>2</sub> tube to 5.7 mm, the same performance specifications were met. The pressure drop was then more than eight times higher than for HFC-134a, and the mass flux and the estimated average heat transfer coefficient were both more than five times higher than for HFC-134a. In practice, and especially when compactness and low mass are essential, the number of tubes should be increased and the diameter further reduced to obtain an optimum design for CO<sub>2</sub>. The CO<sub>2</sub> heat exchangers should be designed for high mass flux, and large pressure drops can be tolerated. In order to save mass and space, the tube diameters should be reduced significantly compared with standard equipment. Efficient heat transfer will compensate for reductions in refrigerant-side surface area. The authors [4] carried out these calculations by integrating estimated local heat transfer and pressure drop data along the tubes.

### **III. PLAIN-FIN AND TUBE EVAPORATOR**

In this paper the authors have presented a program to simulate thermal performance of a cross-counter flow unmixed-unmixed plain fin and tube evaporator. The thermo-physical and transport properties of air and CO<sub>2</sub> are taken from fluid properties database of the Engineering Equation Solver (EES) developed by F-Chart Software. The operating conditions of the evaporator are worked out by transcritical CO<sub>2</sub> cycle simulation considering Indian subtropical conditions and are given in Table 1. The geometrical size of the baseline evaporator is finalized by parametric evaluation at 32°C of air

dry bulb temperature to ensure good performance at even higher ambient temperatures. At these design conditions, the evaporator capacity is expected to be around 2.198 kW.

**Table I: Specifications of the Baseline Evaporator Model**

Parameter	Value	Unit
Face Area	101,250	mm <sup>2</sup>
Evaporator depth ( $L_c$ )	54.0	mm
Number of tube rows ( $N_{tr}$ )	9.0	-
Number of tube columns (in direction of air -flow) ( $N_{tc}$ )	3.0	-
Number of refrigerant circuits ( $N_{crt}$ )	3.0	-
Tube outside diameter ( $D_o$ )	4.7625	mm
Tube thickness ( $\delta_{tube}$ )	0.762	mm
Tube longitudinal pitch ( $P_l$ )	18.0	mm
Tube transverse pitch ( $P_t$ )	25.0	mm
Fin density (FD)	10.0	fins / inch
Fin thickness ( $\delta_{fin}$ )	0.18	mm

**Table II: Operating Conditions of the baseline evaporator model**

Parameter	Value	Unit
Relative humidity of upstream air	50.0	%
Upstream air pressure	1.0	atm
Volume flow rate of air ( $V_h$ )	495.0	m <sup>3</sup> /hr
Refrigerant inlet quality ( $x_{c,i}$ )	0.25	-
Refrigerant mass flow rate ( $m_c$ )	47.0	kg/hr
Refrigerant saturation pressure	41.98	bar
Refrigerant saturation temperature	7.2	°C

**A. Assumptions**

- Steady state heat transfer between the fluids.
- Negligible pressure drop for thermal design calculations.
- No internal heat generation in the evaporator and the heat loss to or from the surroundings is negligible.
- Uniform distribution of refrigerant and air flow.
- Condensation of water vapor in ambient air on evaporator surface is negligible.
- Tube-to-tube conduction through fins is neglected [9], and longitudinal heat conduction is not considered.

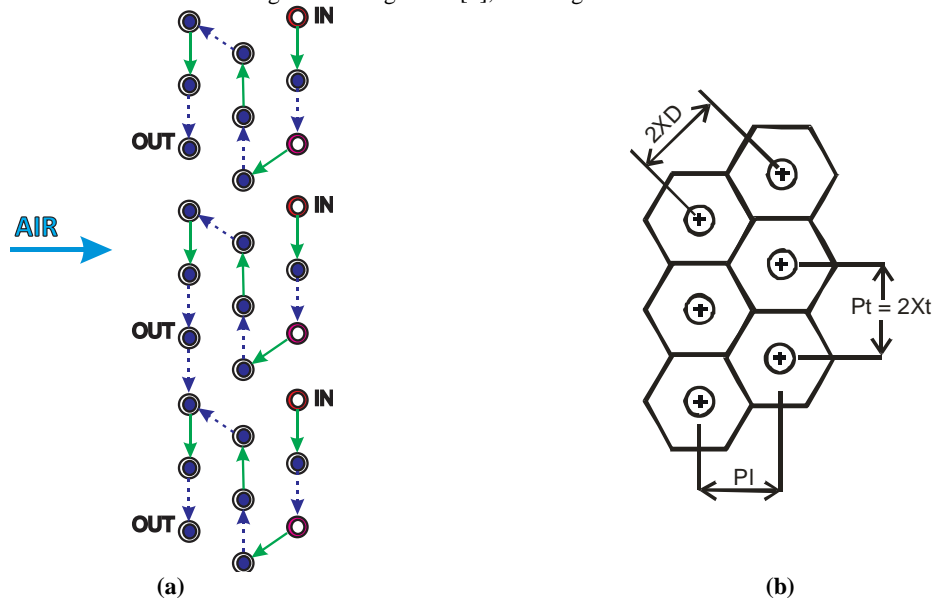


**Fig. 1** Plain-fin and tube evaporator - Staggered tube layout

**IV. METHODOLOGY FOR THE PARAMETRIC SIMULATION**

The parametric simulation of baseline evaporator in consideration is done with the help of Engineering Equation Solver (EES). The details of this simulation are as follows.

The overall conductance UA of the evaporator is inverse of total thermal resistance between refrigerant and air, Rtotal, which can be found by summing all of thermal resistances in series as follows,

$$R_{\text{total}} = \frac{1}{UA} = R_{\text{in}} + R_{\text{f, in}} + R_{\text{cond}} + R_{\text{out}} \quad (1)$$

The resistance between refrigerant and tube inside surface can be represented as,

$$R_{\text{in}} = \frac{1}{\pi D_i W_c N_t \bar{h}_{\text{ref}}} \quad (2)$$

The refrigerant side average heat transfer coefficient  $\bar{h}_{\text{ref}}$  is calculated by using the general flow boiling heat transfer model for evaporation of CO<sub>2</sub> developed by Cheng et al. [5]. The tube inner diameter found as,

$$D_i = D_o - (2 \delta_{\text{tube}}) \quad (3)$$

The total number of tubes is found as,

$$N_t = N_{\text{t,c}} N_{\text{t,r}} \quad (4)$$

The tube wall conduction thermal resistance is found as,

$$R_{\text{cond}} = \frac{\ln \left[ \frac{D_o}{D_i} \right]}{2 \pi W_c N_t k_{\text{tube}}} \quad (5)$$

The resistance between air and the outer surface of the heat exchanger,  $R_{\text{out}}$  can be expressed in terms of an overall surface efficiency,  $\eta_o$ , as follows,

$$R_{\text{out}} = \frac{1}{\eta_o A_{\text{t,2}} \bar{h}_{\text{air}}} \quad (6)$$

where,  $A_{\text{t,2}}$  the total heat transfer surface area available on air side, is the sum of secondary finned surface area  $A_s$ , and primary un-finned tube surface area  $A_p$ . These areas are found as follows,

$$A_p = \pi D_o (W_c - (\delta_{\text{fin}} N_{\text{fin}})) \quad (7)$$

The number of fins is found as,

$$N_{\text{fin}} = \frac{W_c}{P_{\text{fin}}} \quad (8)$$

$$A_s = 2 N_{\text{fin}} \left[ (H_c L_c) - \left( \frac{\pi}{4} D_o^2 N_t \right) \right] \quad (9)$$

Where,  $H_c$  and  $L_c$  are the height and depth of heat exchanger core respectively, are found as,

$$H_c = P_t N_{\text{t,r}} \quad ; \quad L_c = P_1 N_{\text{t,c}} \quad (10)$$

The work of McQuiston and Parker [8] is used to evaluate the air-side convective heat transfer coefficient for a plain-fin and tube heat exchanger with multiple depth-rows of staggered tubes. The model is developed for dry coils. The heat transfer coefficient is based on the Colburn j-factor, which is defined as,

$$j_c = St_h Pr_h^{2/3} \quad (11)$$

Substituting the appropriate values for the Stanton number,  $St_h$ , gives the following relationship for the air-side convective heat transfer coefficient

$$\bar{h}_{\text{air}} = \frac{j_c \dot{G}_h c_{p,h}}{Pr_h^{2/3}} \quad (12)$$

The mass flux of air is found as,

$$\dot{G}_h = \frac{\dot{m}_h}{A_{\text{mf,2}}} \quad (13)$$

$$A_{\text{mf,2}} = (W_c H_c) - (\delta_{\text{fin}} H_c N_{\text{fin}}) - (W_c D_o N_t) \quad (14)$$

where,  $\dot{m}_h$  is the mass flow rate of air, and  $A_{mf,2}$  is minimum free flow area available on air side. McQuiston and Parker [8] used a plain-fin and tube heat exchanger with 4 depth-rows as the baseline model, and for this model defined the Colburn j-factor as,

$$j_{c,4} = 0.2675 (JP) + 1.325 \times 10^{-6} \quad (15)$$

$$JP = Re_{D_o}^{-0.4} \left( \frac{A_{t,2}}{A_t} \right)^{-0.15} \quad (16)$$

where  $A_t$  is the tube outside surface area, and  $A_{t,2}$  is the total air side heat transfer surface area (fin area plus tube area). The Reynolds number,  $Re_{D_o}$  in the above expression is based on the tube outside diameter,  $D_o$ , and the mass flux of air. The area ratio can be expressed as,

$$\frac{A_{t,2}}{A_t} = \frac{4 P_l P_t}{\pi D_h L_c} \sigma \quad (17)$$

The hydraulic diameter  $D_h$ , and  $\sigma$  - the ratio of the minimum free-flow area to the frontal area, are defined as,

$$D_h = \frac{4A_{mf,2}L_c}{A_{t,2}} \quad ; \quad \sigma = \frac{A_{mf,2}}{A_{fr}} \quad (18)$$

The j-factor for heat exchangers with four or fewer depth-rows can then be found using the following correlation,

$$\frac{j_{c,z}}{j_{c,4}} = \frac{1 - 1280(z)(Re_{p1}^{-1.2})}{1 - (1280)(4)(Re_{p1}^{-1.2})} \quad (19)$$

Where,  $z$  is the number of depth-rows of tubes, and  $Re_{p1}$  is the air-side Reynolds number based on the longitudinal tube spacing,

$$Re_{p1} = \frac{\dot{G}_h P_l}{\mu_h} \quad (20)$$

The overall surface efficiency  $\eta_o$  is related to the fin efficiency  $\eta_{fin}$  as follows,

$$\eta_o = 1 - \frac{A_s}{A_{t,2}} (1 - \eta_{fin}) \quad (21)$$

Many experimental studies available in the open literature have been performed in order to characterize the air-side heat transfer performance of several type of fins used in finned tube heat exchangers, and establish correlations which are used for design, rating and modelling of heat exchangers. What is observed in nearly all published papers is that, whatever the fin type (plain, louvered, slit), the fin efficiency calculation is always performed by analytical methods derived from circular fin analysis [11]. The fin efficiency is calculated using Schmidt approximation [11] as follows.

$$\eta_{fin} = \frac{\tanh(m r_o \phi)}{m r_o \phi} \cos(0.1 m r_o \phi) \quad ; \quad m = \sqrt{\frac{2 \bar{h}_{air}}{k_{fin} \delta_{fin}}} \quad (22)$$

$$\phi = \left( \frac{r_f}{r_o} - 1 \right) \left[ 1 + \left( 0.3 + \left( \frac{m(r_f - r_o)}{2.5} \right)^{1.5} \frac{r_f}{12r_o} \left( 0.26 \left( \frac{r_f}{r_o} \right)^{0.3} - 0.3 \right) \right) \ln \left( \frac{r_f}{r_o} \right) \right] \quad (23)$$

$$\frac{r_{f,eq}}{r_o} = 1.27 \frac{X_T}{r_o} \sqrt{\frac{X_D}{X_T} - 0.3} \quad ; \quad 2X_D = \sqrt{P_l^2 + \frac{P_t^2}{4}} = \sqrt{4X_L^2 + X_T^2} \quad (24)$$

The refrigerant side fouling resistance is found as,

$$R_{f,in} = \frac{F_{foul}}{\pi D_i W_c N_t} \quad (25)$$

Where, the refrigerant fouling factor is  $F_{foul}$ . Once, the overall conductance UA of the evaporator is found from eqs. (1), (2), (5), (6), and (25), then number of transfer units NTU is calculated as,

$$NTU = \frac{UA}{C_{min}} \quad (26)$$

$$C_c = \dot{m}_c c_{p,c} \quad ; \quad C_h = \dot{m}_h c_{p,h} \quad (27)$$

$$C_{min} = \begin{cases} C_c & \text{If } C_c < C_h \\ C_h & \text{If } C_h < C_c \end{cases} \quad (28)$$

where,  $C_{min}$  is the minimum heat capacity rate. In evaporation heat transfer analysis, heat capacity rate of the hot fluid is usually taken as the minimum and the heat capacity rate ratio ( $C_r = C_{min}/C_{max}$ ) is zero. The effectiveness  $\varepsilon$  of the evaporator and the evaporator cooling capacity are respectively found as given in equations 29 and 30.

$$\varepsilon = 1 - e^{(-NTU)} \quad (29)$$

$$\dot{Q}_{ev} = \varepsilon C_{min} (T_{h,i} - T_{c,i}) \quad (30)$$

Then, outlet temperature of hot fluid  $T_{h,o}$  is found from the heat balance mentioned in equation 31 as,

$$\dot{Q}_{ev} = C_h (T_{h,i} - T_{h,o}) \quad (31)$$

The enthalpy of refrigerant at outlet  $h_{c,o}$  is found from the knowledge of heat balance on refrigerant side as follows,

$$\dot{Q}_{ev} = \dot{m}_c |h_{c,i} - h_{c,o}| \quad (32)$$

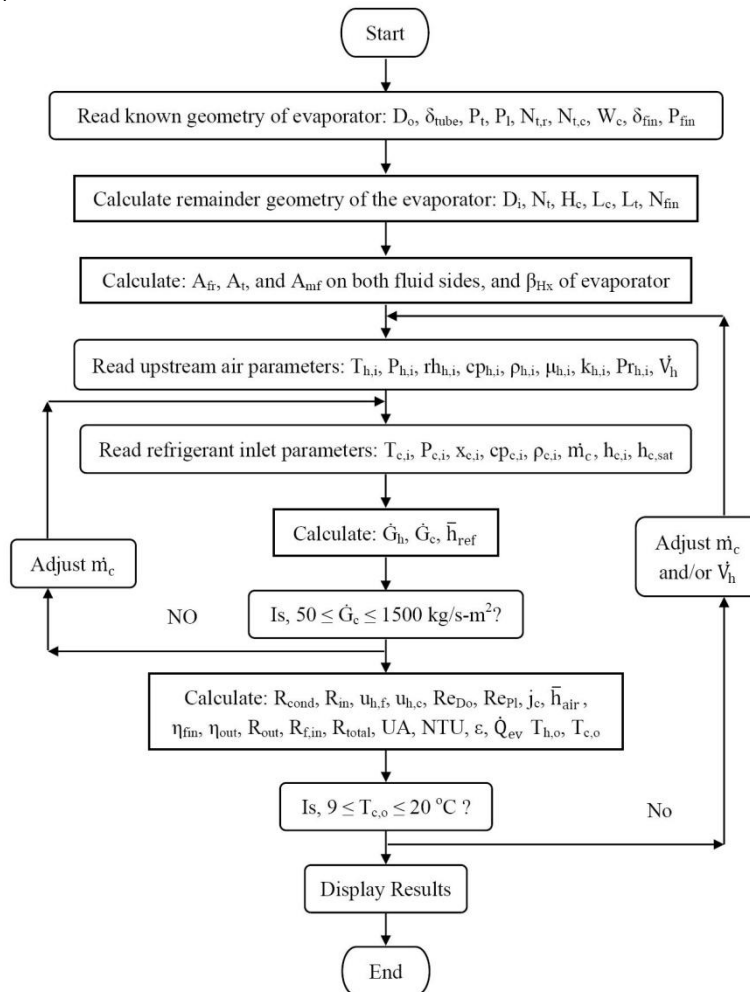


Fig. 2 Simulation flowchart

The refrigerant enthalpy at outlet is compared with the saturation enthalpy  $h_{c,sat}$  of refrigerant. If ( $h_{c,o} < h_{c,sat}$ ), the refrigerant is still in the two-phase region. In such a case mass flow rate of refrigerant and/or volume flow rate of air is adjusted till the refrigerant at outlet is in superheated vapor condition. If ( $h_{c,o} > h_{c,sat}$ ), the refrigerant is in superheat region. The temperature of superheated refrigerant at evaporator exit is calculated from equation below,

$$h_{c,o} = h_{c,sat} + cp_c (T_{c,o} - T_{c,sat}) \quad (33)$$

In above equation,  $h_{c,sat}$  and  $T_{c,sat}$  are enthalpy and temperature of refrigerant vapour, and the only unknown is outlet temperature of refrigerant  $T_{c,o}$ .

In this way, the capacity of evaporator for given geometry and thermo-physical properties of the fluids, is calculated using Effectiveness-NTU method of heat exchanger design. The details of thermal design of evaporator are briefly explained in form of a flowchart as given in Figure 2.

## V. RESULTS AND DISCUSSIONS

The thermal design of the plain-fin and tube evaporator using CO<sub>2</sub> as a refrigerant is done as per the procedure outlined in the Figure 2. The geometry parameters such as fin density, fin thickness, tube-longitudinal and transverse pitch etc., significantly affect overall performance of a plain-fin and tube heat exchanger. Even if any one of the aforementioned geometry parameters is wrongly selected, the performance evaluation of plain-fin and tube heat exchanger will be erroneous. Hence, geometry of the evaporator is fine tuned for its maximum energy performance at design operating conditions, considering the acceptable ranges of the aforementioned geometry parameters.

### A. Effect of Fin density

Fin density is important in achieving the desired secondary surface area on the air side and compactness of the heat exchanger. Normally, fin densities for plain-fins vary from 250 - 800 fins/m (6 - 20 fpi). The effect of change in fin density on performance of plain-fin and tube evaporator is studied using fin densities in the range of 8-12 fpi. The effect of change in fin density on Colburn j-factor with respect to change in air-side Reynolds number based on tube longitudinal pitch  $Re_{p1}$ , for varying air flow rate, is depicted in Figure 3.

For 495 m<sup>3</sup>/hr of air flow rate at 32°C air inlet temperature, 50% increase in fin density from 8-12 fpi, gives 7.62% decrease in air-side minimum free flow. This gives an increase in air-side Reynolds number  $Re_{p1}$  by 8.24% and 9.37% decrease in Colburn j-factor as given in Figure 3. It is also observed from Figure 3 that, for fin density of 10 fpi, with 4.21% increase in air flow rate from 475 - 495 m<sup>3</sup>/hr, Colburn j-factor decreases by 2.06% for an increase of 4.23% in air-side Reynolds number  $Re_{p1}$ .

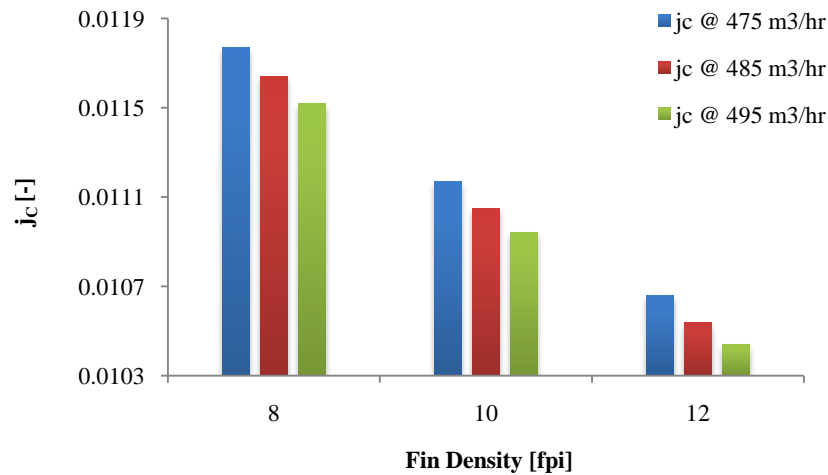


Fig. 3 Effect of fin density on Colburn j-factor

### B. Effect of Fin thickness

The effect of change in fin thickness on Colburn j-factor, with respect to change in Reynolds number of air  $Re_{p1}$ , for varying air flow rate, is shown in Figure 4.

Fin thickness,  $\delta_{fin}$ , is yet another important geometry parameter to be carefully selected in the design of plain-fin and tube heat exchangers. This is because; wrongly selected value of fin thickness can adversely affect the capacity of a plain-fin and tube heat exchanger. Normally, for a plain-fin and tube heat exchanger, fin thicknesses vary from 0.08 to 0.25 mm (0.003 to 0.010 in.). The fin thickness values considered for this study are in the range of 0.14 mm to 0.22 mm.

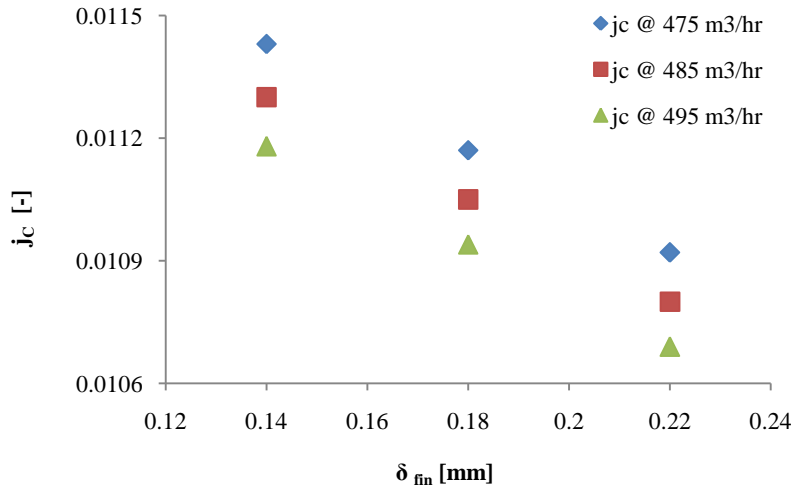


Fig. 4 Fin thickness v/s Colburn j-factor

At 495 m<sup>3</sup>/hr of air flow rate, for 57.14% increase in fin thickness from 0.14 to 0.22 mm, air-side minimum free flow area reduces by 8.41% and Reynolds number of air,  $Re_{pi}$  increases by 9.22%. Hence, Colburn j-factor decreases by 4.38%, as shown in Figure 4. It can also be seen in Figure 4 that, for fin thickness of 0.18 mm, due to increase in air flow rate from 475 - 495 m<sup>3</sup>/hr, Reynolds number of air  $Re_{pi}$  increases by 4.23%, and consequently Colburn j-factor decreases by 2.06%.

**C. Effect of Tube Longitudinal Pitch**

Figure 5 represents the effect of change in tube longitudinal pitch on Colburn j-factor, with respect to change in Reynolds number of air  $Re_{pi}$ , for varying air flow rate. As studied by Romero-Méndez et al. [9], at very low values of tube longitudinal pitch, tube to tube conduction through fins will be considerable degrading the performance of plain-fin and tube heat exchangers. Typically, for plain-fin and tube heat exchangers, tube longitudinal pitch is selected such that fin flow length is achieved from 25 to 250 mm. For the present study, the tube longitudinal pitches in the range of 18 to 22 mm giving fin flow lengths between 54 to 66 mm are selected.

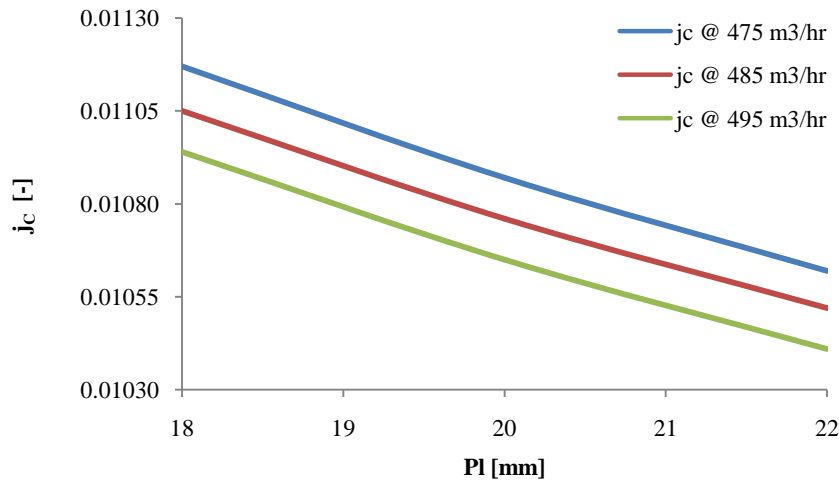


Fig. 5 Tube longitudinal pitch v/s Colburn-j factor

For 22.22% increase in tube longitudinal pitch from 18 to 22 mm at 495 m<sup>3</sup>/hr of air flow rate, Reynolds number of air  $Re_{pi}$  increases by 22.2%. Consequently, Colburn j-factor decreases by 4.84% as seen in Figure 5. On the contrary, for tube longitudinal pitch of 18 mm, with increase in air flow rate from 475 - 495 m<sup>3</sup>/hr, the mass flux of air and Reynolds number of air  $Re_{pi}$  increase by 4.25 and 4.26 % respectively. Due to this, Colburn j-factor decreases by 2.06% as observed in Figure 5.

**D. Effect of Tube transverse pitch**

The effect of change in tube transverse pitch on Colburn j-factor, with respect to change in air-side Reynolds number based on tube outside diameter,  $Re_{Do}$ , for varying air flow rate, is graphically represented in Figure 6. At lower values of tube transverse pitch  $P_t$ , average air velocity and the Reynolds number will be on higher side producing un-

necessary turbulence. Similarly, the air-side pressure drop tends to increase in inverse proportion with tube transverse pitch. At higher values of tube transverse pitches, the air-side pressure drop reduces, but the performance of plain-fin and tube heat exchangers degrades. So, tube transverse pitch should be carefully selected. In this study, the tube transverse pitches in the range of 21 to 25 mm are considered.

At 495 m<sup>3</sup>/hr of air flow rate, for 19.04% increase in tube transverse pitch from 21 to 25 mm, air-side minimum free flow area increases by 71.12%. Due to this, the Reynolds number of air  $Re_{D_o}$  reduces by 41.6%. Hence, Colburn j-factor increases by 25.7% in direct proportion with tube transverse pitch, as depicted in Figure 6.

On the contrary, for 25 mm of tube transverse pitch, with 4.21% increase in air flow rate from 475 - 495 m<sup>3</sup>/hr, mass flux of air and Reynolds number of air  $Re_{D_o}$  increase by 4.25 and 4.21% respectively. Hence, Colburn j-factor decreases by 2.06% with increase in air flow rate, as observed in Figure 6.

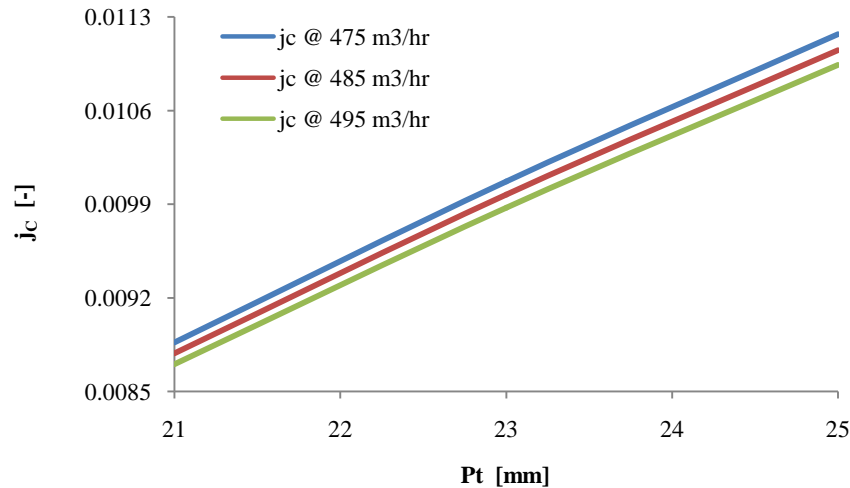


Fig. 6 Variation in Colburn j-factor with change in tube transverse pitch

## VI. CONCLUSIONS

- Global warming and climate change being an alarming issue, the culprits - synthetic refrigerants-CFCs, HCFCs, HFCs, etc needed to be phased out. This has led to increase in use of 'Natural' refrigerants. Among the 'Natural' refrigerants, CO<sub>2</sub> stands out as more eco-friendly contender.
- CO<sub>2</sub> heat exchangers should be designed for high mass flux, and large pressure drops are tolerable. For compactness, the tube diameters should be reduced significantly compared with standard equipment. Despite reduction in refrigerant-side surface area, heat transfer will be efficient owing to high heat transfer coefficients and high volumetric heat capacity of CO<sub>2</sub>.
- The model proposed in this study, based on Effectiveness-NTU method of heat exchanger design, can prove to be a simple yet effective tool for studying thermal design of plain-fin and tube heat exchangers.
- The geometry of baseline evaporator is fine tuned for maximum performance at design operating conditions by parametric optimization of geometry parameters avoiding any major loss in capacity at elevated ambient temperatures.
- For a given air flow rate, the Colburn-j factor decreases by 4.5 to 5.1% with every 2 fpi increase in fin density from 8 to 12 fpi, and for a given fin density, with every 10 m<sup>3</sup>/hr increase in air flow rate from 475 - 495 m<sup>3</sup>/hr, Colburn j-factor decreases by 1.0 to 1.1%.
- For a given air flow rate, Colburn-j factor decreases by approximately 2.25% for 0.02 mm increase in fin thickness from 0.14 to 0.22 mm. While for a given fin thickness, due to every 10 m<sup>3</sup>/hr increase in air flow rate from 475 - 495 m<sup>3</sup>/hr, Colburn j-factor decreases by approximately 1.0 - 1.1%.
- At a given air flow rate, with every 2 mm increase in tube longitudinal pitch from 18 to 22 mm, Colburn j-factor decreases by approximately 2.45%. On the contrary, for a given tube longitudinal pitch, with every 10 m<sup>3</sup>/hr increase in air flow rate from 475 - 495 m<sup>3</sup>/hr, Colburn j-factor decreases by roughly 1.0%.
- For a given air flow rate, with every 2 mm increase in tube transverse pitch from 21 to 25 mm, Colburn j-factor increases by about 10.5 - 13.5% in direct proportion with tube transverse pitch. However, for a given tube transverse pitch, with every 10 m<sup>3</sup>/hr increase in air flow rate from 475 - 495 m<sup>3</sup>/hr, Colburn j-factor decreases only by 1.0 - 1.1% approximately.
- As discussed above, for effective cooling of air, geometry of the plain-fin and tube evaporator is optimized for better heat transfer coefficient on air side without losing out on overall compactness of the heat exchanger. The geometry of CO<sub>2</sub> evaporator (as given in Table 3) is thus finalized by parametric optimization for effective cooling of air. The evaporator designed can deliver about 2.2 kW of cooling effect while achieving compactness of 787 m<sup>2</sup>/m<sup>3</sup> of core volume.

### **List of Symbols and Abbreviations**

#### **Symbols**

$A_{fr}$	Frontal area [m <sup>2</sup> ]
$A_{mf}$	Minimum free flow area [m <sup>2</sup> ]
$A_p$	Primary (un-finned) surface area [m <sup>2</sup> ]
$A_s$	Secondary (finned) surface area [m <sup>2</sup> ]
$A_t$	Total area [m <sup>2</sup> ]
$\beta_{Hx}$	Surface area density of the evaporator [m <sup>2</sup> m <sup>-3</sup> ]
$C$	Heat capacity rate [W K <sup>-1</sup> ]
$c_f$	Ratio of effective fin radius to tube outer radius [-]
$cp$	Specific heat capacity [J kg <sup>-1</sup> K <sup>-1</sup> ]
$D_i$	Tube inside diameter [m]
$D_o$	Tube outside diameter [m]
$f$	Friction factor [-]
$FD$	Fin density [fins inch <sup>-1</sup> or fpi]
$F_{foul}$	Refrigerant fouling factor [m <sup>2</sup> K W <sup>-1</sup> ]
$\dot{G}$	Mass flux [kg s <sup>-1</sup> m <sup>-2</sup> ]
$\bar{h}$	Average heat transfer coefficient [W m <sup>-2</sup> K <sup>-1</sup> ]
$h$	Enthalpy [J kg <sup>-1</sup> ]
$H_c$	Evaporator height [m]
$j_c$	Colburn j-factor [-]
$k$	Thermal conductivity [W m <sup>-1</sup> K <sup>-1</sup> ]
$L_c$	Evaporator depth [m]
$L_t$	Total tube length [m]
$N_{fin}$	Number of fins [-]
$N_t$	Total number of tubes [-]
$N_{t,c}$	Number of tube columns [-]
$N_{t,r}$	Number of tube rows [-]
$P$	Pressure [bar]
$P_{fin}$	Fin spacing/pitch [m]
$P_l$	Tube longitudinal spacing [m]
$Pr$	Prandtl number [-]
$P_t$	Tube transverse spacing [m]
$\dot{Q}_{ev}$	Evaporator capacity [W]
$R$	Thermal resistance [C W <sup>-1</sup> ]
$Re$	Reynolds number [-]
$UA$	Thermal conductance [W C <sup>-1</sup> ]
$\dot{V}$	Volume flow rate [m <sup>3</sup> s <sup>-1</sup> ]
$W_c$	Evaporator length [m]

#### **Greek Letters**

$\varepsilon$	Evaporator heat exchange effectiveness [%]
$\delta$	Thickness [m]
$\eta$	Efficiency [%]
$\rho$	Density [kg m <sup>-3</sup> ]

#### **Subscripts**

$c$	Evaporator core dimensions
$c, 1$	Cold fluid (refrigerant) parameters
$h, 2$	Hot fluid (air) parameters
$i$	Inlet conditions
$o$	Outlet conditions

### **REFERENCES**

- [1]. Alberto Cavallini, *Properties of CO<sub>2</sub> as a refrigerant, European Seminar – CO<sub>2</sub> as a Refrigerant*, Galileo Industry Training & Education Center, University of London Research Center for Environment and Business.
- [2]. G. Lorentzen, "The Use of Natural Refrigerants: A Complete Solution to the CFC/HCFC Predicament", *International Journal of Refrigeration*, 18 (3), pp. 190-197, 1995.
- [3]. Roland Handschuh, *Design Criteria for CO<sub>2</sub> Evaporators*, Paper for GTZ Proklima, published in 'Natural Refrigerants – sustainable ozone- and climate friendly alternatives to HCFCs', April 2008, pp. 1-7.
- [4]. J. Pettersent et. al., "Development of compact heat exchangers for CO<sub>2</sub> air-conditioning systems", *International Journal of Refrigeration*, 2 (3), pp. 180-193, 1998.
- [5]. L. Cheng, et. al., "New flow boiling heat transfer model and flow pattern map for carbon dioxide evaporating inside horizontal tubes", *International Journal of Heat and Mass Transfer*, 49, pp. 4082–4094, 2006.
- [6]. L. Cheng et. al., "New prediction methods for CO<sub>2</sub> evaporation inside tubes: Part I - A two-phase flow pattern map and a flow pattern based phenomenological model for two-phase flow frictional pressure drops", *International Journal of Heat and Mass Transfer*, 51, pp. 111-124, 2008.

- [7]. L. Cheng, et. al., “New prediction methods for CO<sub>2</sub> evaporation inside tubes: Part II – An updated general flow boiling heat transfer model based on flow patterns”, *International Journal of Heat and Mass Transfer*, 51, pp. 125-135, 2008.
- [8]. C. C. Wang and K. Y. Chi, “Heat transfer and friction characteristics of plain fin-and-tube heat exchangers, Part I: new experimental data”, *International Journal of Heat and Mass Transfer*, 43, pp. 2681-2691, 2000.
- [9]. M.F. Wright, “Plate-fin-and-tube Condenser Performance and Design for refrigerant R410a Air-Conditioner”, M.S. thesis, Georgia Institute of Technology, USA, May 2000.
- [10]. R. Romero-Méndez et. al., “Effect of tube-to-tube conduction on plate-fin and tube heat exchanger performance”, *International Journal of Heat and Mass Transfer*, 40 (16), pp. 3909 -3916, 1997.
- [11]. S.W. Stewart, “Enhanced finned-tube condenser design and optimization”, PhD Thesis, Georgia Institute of Technology, USA, November 2003.
- [12]. T. Perrotin and D. Clodic, *Fin Efficiency Calculation in Enhanced Fin-and-Tube Heat Exchangers in Dry Conditions*, International Congress of Refrigeration, Washington, D.C., pp. 1-8, 2003.
- [13]. J.R. Thome, Chapter 13: Two phase pressure drops, Wolverine Engineering Data Book III.